

HIGHER-ORDER SEMI-RATIONAL SOLUTIONS FOR THE COUPLED COMPLEX MODIFIED KORTEWEG-DE VRIES EQUATION

YU LOU, YI ZHANG*  AND RUSUO YE

Abstract. We explore the Darboux-dressing transformation of the coupled complex modified Korteweg-de Vries equation. Next, with the aid of an asymptotic expansion theory, we derive the concrete forms of three types of semi-rational solutions. In particular, the seed solution is related to the normalized distance and retarded time. Interestingly, we construct a kind of novel rogue wave called as curve rogue wave. More importantly, the kinetics of semi-rational solutions are discussed in detail. We hope that these results would shed more light on comprehending of the solutions occurring in multi-component coupled systems.

Mathematics Subject Classification. 35Q51/37K40/74H05.

Received August 26, 2021. Accepted January 28, 2022.

1. INTRODUCTION

Rogue waves with high amplitudes have become a fashionable research in various realms such as science, oceanic waves, optics and even finance [3, 6, 22, 27]. Besides, rogue waves appear and disappear both from nowhere [1]. Taking into account the adhibition of different domains needs us to study the rogue wave of nonlinear evolution equations to understand its behaviors. It should be emphasized that breather waves are divided into two kinds which tend to become rogue waves [2, 12, 13, 21].

From in physics viewpoint, the interaction of semi-rational solutions composed of the rogue wave and the soliton or breather in integrable systems catch the attention of academics. Since Ling *et al.* constructed the rational solutions in vector nonlinear Schrödinger (NLS) equations [15], the localized wave solutions in other nonlinear integrable equations, for instance, coupled Hirota equations [23], coupled Lakshmanan-Pereszian-Daniel equations [25], coupled derivative NLS equation [26] and the Hirota-Maccari system [24] have been presented. Notably, Darboux transformation (DT) is an essential method to obtain soliton and localized solutions of soliton equations [9, 17, 18, 29–31]. Recently, a new method is presented to obtain the localized wave solutions of integrable equations, namely, Darboux-dressing transformation (DDT) [4, 5, 20].

The modified Korteweg-de Vries (mKdV) equation, as everyone knows, is a fundamental completely integrable equation which plays a significant role in various physical contexts [11, 14, 16]. Another integrable equation

Keywords and phrases: Coupled complex modified Korteweg-de Vries equation, Darboux-dressing transformation, semi-rational solutions.

Department of Mathematics, Zhejiang Normal University, Jinhua 321004, PR China.

* Corresponding author: zy2836@163.com

is the complex mKdV equation with a large number of applications [7, 10]. It can be found that results in multi-component systems are more plentiful than ones in single systems.

In this work, one aims to study the coupled complex modified Korteweg-de Vries (ccmKdV) equation

$$\begin{aligned} u_{1t} + u_{1xxx} + 3(|u_1|^2 + |u_2|^2)u_{1x} + 3(u_{1x}u_1^* + u_{2x}u_2^*)u_1 &= 0, \\ u_{2t} + u_{2xxx} + 3(|u_1|^2 + |u_2|^2)u_{2x} + 3(u_{1x}u_1^* + u_{2x}u_2^*)u_2 &= 0, \end{aligned} \quad (1.1)$$

where $u_1 = u_1(x, t)$, $u_2 = u_2(x, t)$ are complex functions and the symbol $*$ denotes the complex conjugation. It is noticed that algebro-geometric solutions and N -soliton solutions have been obtained [8, 19]. Beyond that, Ye *et al.* gave the modulation instability and vector rogue waves [28].

This study is committed to investigating semi-rational solutions. In Section 2, in the light of the Lax pair, we give the DDT method. In Section 3, with the aid of the asymptotic expansion method, the higher-order semi-rational solutions are presented. Peculiarly, one gains a kind of the novel rogue wave with curve shape. Moreover, the kinetics of these solutions are discussed. The conclusion is situated on the final section.

2. DARBOUX-DRESSING TRANSFORMATION

The Lax pair of equation (1.1) is written by

$$\begin{aligned} \Psi_x &= U\Psi, \quad U = \frac{1}{2}i\lambda\sigma + i\sigma Q, \\ \Psi_t &= V\Psi, \quad V = \frac{1}{2}i\lambda^3\sigma + i\lambda^2\sigma Q + \lambda V_1 + V_0, \end{aligned} \quad (2.1)$$

with

$$\begin{aligned} V_1 &= i\sigma Q^2 + Q_x, \quad V_0 = Q_x Q - Q Q_x + 2i\sigma Q^3 - i\sigma Q_{xx}, \\ \sigma &= \begin{pmatrix} 1 & 0 & 0 \\ 0 & -1 & 0 \\ 0 & 0 & -1 \end{pmatrix}, \quad Q = \begin{pmatrix} 0 & u_1 & u_2 \\ -u_1^* & 0 & 0 \\ -u_2^* & 0 & 0 \end{pmatrix}, \end{aligned}$$

where Ψ indicates the eigenfunction and λ is a spectral parameter. From the zero curvature equation $U_t - V_x + [U, V] = 0$, one can easily obtain equation (1.1).

Then, one gives the DDT of the ccmKdV equation (1.1) in the following

$$D[1] = I - \frac{\lambda_1 - \lambda_1^*}{\lambda - \lambda_1^*} P_1, \quad P_1 = \frac{\hat{\Phi}_0 \hat{\Phi}_0^\dagger}{\hat{\Phi}_0^\dagger \hat{\Phi}_0}, \quad (2.2)$$

where $I = \text{diag}(1, 1, 1)$ and $\hat{\Phi}_0(x, t) = (\hat{\phi}_1, \hat{\phi}_2, \hat{\phi}_3)^T$. Then the new functions read

$$\begin{pmatrix} u_{1,[1]} \\ u_{2,[1]} \end{pmatrix} = \begin{pmatrix} u_{1,[0]} \\ u_{2,[0]} \end{pmatrix} + \frac{(\lambda_1 - \lambda_1^*)\hat{\phi}_1}{|\hat{\phi}_1|^2 + |\hat{\phi}_2|^2 + |\hat{\phi}_3|^2} \begin{pmatrix} \hat{\phi}_2^* \\ \hat{\phi}_3^* \end{pmatrix}. \quad (2.3)$$

Theorem 2.1. *Let $\Psi[\lambda_1(1 + \epsilon)]$ be a solution of (2.1) with $\lambda = \lambda_1(1 + \epsilon)$ and an initial solution $\begin{pmatrix} u_{1,[0]} \\ u_{2,[0]} \end{pmatrix}$. If $\Psi[\lambda_1(1 + \epsilon)]$ can be expanded at λ_1*

$$\Psi[\lambda_1(1 + \epsilon)] = \Psi_0 + \Psi_1\epsilon + \Psi_2\epsilon^2 + \dots, \quad (2.4)$$

then

$$\begin{aligned}\hat{\Phi}_{[n]} &= \begin{pmatrix} \hat{\phi}_{1,[n]} \\ \hat{\phi}_{2,[n]} \\ \hat{\phi}_{3,[n]} \end{pmatrix} = \lambda_1 \hat{\Phi}_{[n-1]} + D[n] \hat{\Xi}_{[n]}, \quad n \in Z_+, \\ \hat{\Phi}_{[0]} &= \begin{pmatrix} \hat{\phi}_{1,[0]} \\ \hat{\phi}_{2,[0]} \\ \hat{\phi}_{3,[0]} \end{pmatrix} = \Psi_0, \\ \hat{\Xi}_{[n]} &= \hat{\Phi}_{[n]} (\Psi_{j+1} \rightarrow \Psi_{j+2}), \quad j = 0, 1, 2, \dots,\end{aligned}\tag{2.5}$$

with

$$D[n] = (\lambda - \lambda_1^*)I + (\lambda_1^* - \lambda_1) \frac{\hat{\Phi}_{[n-1]} \hat{\Phi}_{[n-1]}^\dagger}{\hat{\Phi}_{[n-1]}^\dagger \hat{\Phi}_{[n-1]}},\tag{2.6}$$

are solutions of (2.1) with respect to the same spectral parameter λ_1 .

Then the solution $\begin{pmatrix} u_{1,[n]} \\ u_{2,[n]} \end{pmatrix}$ reads as

$$\begin{pmatrix} u_{1,[n]} \\ u_{2,[n]} \end{pmatrix} = \begin{pmatrix} u_{1,[n-1]} \\ u_{2,[n-1]} \end{pmatrix} + \frac{(\lambda_1 - \lambda_1^*) \hat{\phi}_{1,[n-1]}}{|\hat{\phi}_{1,[n-1]}|^2 + |\hat{\phi}_{2,[n-1]}|^2 + |\hat{\phi}_{3,[n-1]}|^2} \begin{pmatrix} \hat{\phi}_{2,[n-1]} \\ \hat{\phi}_{3,[n-1]} \end{pmatrix}.\tag{2.7}$$

Afterwards, we begin with the initial solution

$$u_{j,[0]} = a_j e^{i\theta}, \quad \theta = kx + \varpi t, \quad j = 1, 2,\tag{2.8}$$

where a_j , k and ϖ are real constants. After the simple calculation, we can get the dispersion relation

$$\varpi = k^3 - 6k(a_1^2 + a_2^2).\tag{2.9}$$

3. HIGHER-ORDER SEMI-RATIONAL SOLUTIONS

By adopting the resulting DDT, we painlessly achieve the higher-order semi-rational solutions. Firstly, substituting the following transformation

$$\Psi = \mathcal{A}\Phi, \quad \mathcal{A} = \begin{pmatrix} 1 & 0 & 0 \\ 0 & e^{-i\theta} & 0 \\ 0 & 0 & e^{-i\theta} \end{pmatrix},\tag{3.1}$$

into the Lax pair (2.1), we can get that

$$\begin{aligned}\Phi_x &= [\mathcal{A}^{-1}U\mathcal{A} + (\mathcal{A}^{-1})_x\mathcal{A}]\Phi = iU_0\Phi, \\ \Phi_t &= [\mathcal{A}^{-1}V\mathcal{A} + (\mathcal{A}^{-1})_t\mathcal{A}]\Phi = iV_0\Phi,\end{aligned}\tag{3.2}$$

with

$$U_0 = \begin{pmatrix} \frac{\lambda}{2} & a_1 & a_2 \\ a_1 & -\frac{\lambda}{2} + k & 0 \\ a_2 & 0 & -\frac{\lambda}{2} + k \end{pmatrix}, \quad (3.3)$$

$$V_0 = (\lambda + 2k)U_0^2 + (\lambda^2 - k^2 - 2\omega^2)U_0 - \left(\frac{\lambda^3}{4} + \frac{k}{2}\lambda^2 - \frac{2k^2 - 4\omega^2}{4}\lambda + 4k\omega^2\right), \quad (3.4)$$

and $\omega^2 = a_1^2 + a_2^2$, where Φ is a 3×3 matrix function of x and t , U_0 and V_0 are both the 3×3 constant matrices. Thus, the solution for system (2.1) can be written as

$$\left(\hat{\phi}_1, \hat{\phi}_2, \hat{\phi}_3\right)^T = \mathcal{A}\mathcal{F}\mathcal{G}\mathcal{Z}, \quad \mathcal{F} = e^{iU_0x}, \quad \mathcal{G} = e^{iV_0t}, \quad (3.5)$$

and $\mathcal{Z} = (\mu_1, \mu_2, \mu_3)^T$ is a free vector.

After complicated calculations, \mathcal{F} can be written by

$$\mathcal{F} = \frac{1}{\varsigma} e^{\frac{ik}{2}x} \begin{pmatrix} \Lambda_1 & \Lambda_2 & \Lambda_3 \\ \Lambda_2 & \Lambda_4 & \Lambda_5 \\ \Lambda_3 & \Lambda_5 & \Lambda_6 \end{pmatrix}, \quad (3.6)$$

where

$$\begin{aligned} \Lambda_1 &= \varsigma \cos\left(\frac{\varsigma}{2}x\right) + i(\lambda - k) \sin\left(\frac{\varsigma}{2}x\right), \\ \Lambda_2 &= 2ia_1 \sin\left(\frac{\varsigma}{2}x\right), \\ \Lambda_3 &= 2ia_2 \sin\left(\frac{\varsigma}{2}x\right), \\ \Lambda_4 &= \frac{a_1^2}{\omega^2} \left(\varsigma \cos\left(\frac{\varsigma}{2}x\right) - i(\lambda - k) \sin\left(\frac{\varsigma}{2}x\right)\right) + \frac{a_2^2}{\omega^2} \varsigma e^{-\frac{i(\lambda-k)}{2}x}, \\ \Lambda_5 &= \frac{a_1 a_2}{\omega^2} \left(\varsigma \cos\left(\frac{\varsigma}{2}x\right) - i(\lambda - k) \sin\left(\frac{\varsigma}{2}x\right)\right) - \frac{a_1 a_2}{\omega^2} \varsigma e^{-\frac{i(\lambda-k)}{2}x}, \\ \Lambda_6 &= \frac{a_2^2}{\omega^2} \left(\varsigma \cos\left(\frac{\varsigma}{2}x\right) - i(\lambda - k) \sin\left(\frac{\varsigma}{2}x\right)\right) + \frac{a_1^2}{\omega^2} \varsigma e^{-\frac{i(\lambda-k)}{2}x}, \\ \omega^2 &= a_1^2 + a_2^2, \quad \varsigma = \sqrt{(\lambda - k)^2 + 4\omega^2}. \end{aligned}$$

Likewise, \mathcal{G} can read as

$$\mathcal{G} = \frac{1}{\varrho} e^{\frac{i\varpi}{2}t} \begin{pmatrix} \Omega_1 & \Omega_2 & \Omega_3 \\ \Omega_2 & \Omega_4 & \Omega_5 \\ \Omega_3 & \Omega_5 & \Omega_6 \end{pmatrix}, \quad (3.7)$$

where

$$\begin{aligned}
\Omega_1 &= \varrho \cos\left(\frac{\varrho}{2}t\right) + i\mu \sin\left(\frac{\varrho}{2}t\right), \\
\Omega_2 &= 2ia_1\nu \sin\left(\frac{\varrho}{2}t\right), \\
\Omega_3 &= 2ia_2\nu \sin\left(\frac{\varrho}{2}t\right), \\
\Omega_4 &= \frac{a_1^2}{\omega^2}(\varrho \cos\left(\frac{\varrho}{2}t\right) - i\mu \sin\left(\frac{\varrho}{2}t\right)) + \frac{a_2^2}{\omega^2}\varrho e^{-it\left(\frac{\lambda^3}{2} - \frac{k^3}{2} + 3k\omega^2\right)}, \\
\Omega_5 &= \frac{a_1a_2}{\omega^2}(\varrho \cos\left(\frac{\varrho}{2}t\right) - i\mu \sin\left(\frac{\varrho}{2}t\right)) - \frac{a_1a_2}{\omega^2}\varrho e^{-it\left(\frac{\lambda^3}{2} - \frac{k^3}{2} + 3k\omega^2\right)}, \\
\Omega_6 &= \frac{a_2^2}{\omega^2}(\varrho \cos\left(\frac{\varrho}{2}t\right) - i\mu \sin\left(\frac{\varrho}{2}t\right)) + \frac{a_1^2}{\omega^2}\varrho e^{-it\left(\frac{\lambda^3}{2} - \frac{k^3}{2} + 3k\omega^2\right)}, \\
\varrho &= (\lambda^2 + k\lambda + k^2 - 2\omega^2)\varsigma, \\
\mu &= \lambda^3 - 2\omega^2\lambda + 2k\omega^2 - k^3, \\
\nu &= \lambda^2 + k\lambda + k^2 - 2\omega^2.
\end{aligned}$$

Substituting the seed solution (2.8) into the DDT (2.3) results in explicit solutions composed of trigonometric functions and exponential functions. In what follows, the asymptotic expansion theory will be employed to construct the rational solutions. When we set $\lambda = k \pm 2i\omega$, the exponential $e^{i(U_0x + V_0t)}$ can be regarded as consisting of two parts: exponential and polynomial functions. Setting $\lambda = (k + 2i\omega)(1 + \epsilon)$, one can give a theorem as below.

Theorem 3.1. *Taking into account a Taylor series expansion in (2.3) and (3.5), we have the following expressions*

$$\begin{aligned}
\mathcal{F}|_{\lambda=(k+2i\omega)(1+\epsilon)} &= e^{\frac{ik}{2}x} \sum_{n=0}^{\infty} \mathcal{F}_n \epsilon^n, \\
\mathcal{G}|_{\lambda=(k+2i\omega)(1+\epsilon)} &= e^{\frac{i(k^3-6k\omega^2)}{2}t} \sum_{n=0}^{\infty} \mathcal{G}_n \epsilon^n,
\end{aligned} \tag{3.8}$$

where \mathcal{F}_n and \mathcal{G}_n represent n th coefficient matrix of ϵ . And \mathcal{Z} reads

$$\mathcal{Z} = \sum_{j=0}^{\infty} \mathcal{Z}_j \epsilon^j, \tag{3.9}$$

here \mathcal{Z}_j are constant vectors. Consequently, one gains

$$\Psi = \sum_{n=0}^{\infty} \Psi_n \epsilon^n, \quad \Psi_n = e^{i\left(\frac{k}{2}x + \frac{(k^3-6k\omega^2)}{2}t\right)} \mathcal{A} \sum_{k=0}^n \sum_{j=0}^n \mathcal{F}_k \mathcal{G}_j \mathcal{Z}_{n-k-j}. \tag{3.10}$$

Additionally, to divide the rational solutions, \mathcal{Z} allows the following expression

$$\mathcal{Z} = \sum_{k=0}^{\infty} \mathcal{Z}_k \epsilon^k = e^{i(U_0|_{\lambda=(k+2i\omega)(1+\epsilon)}X + V_0|_{\lambda=(k+2i\omega)(1+\epsilon)}T)} p, \tag{3.11}$$

with

$$X = \sum_{n=0}^{\infty} R_n \epsilon^n, \quad T = \sum_{n=0}^{\infty} S_n \epsilon^n, \quad p = (p_1, p_2, p_3)^T. \quad (3.12)$$

Therefore, the first-order semi-rational solutions are generated

$$\begin{pmatrix} q_{1,[1]} \\ q_{2,[1]} \end{pmatrix} = e^{i\theta} \begin{pmatrix} a_1 \\ a_2 \end{pmatrix} + \frac{4i\omega \hat{\phi}_{1,[0]}}{|\hat{\phi}_{1,[0]}|^2 + |\hat{\phi}_{2,[0]}|^2 + |\hat{\phi}_{3,[0]}|^2} \begin{pmatrix} \hat{\phi}_{2,[0]}^* \\ \hat{\phi}_{3,[0]}^* \end{pmatrix}, \quad (3.13)$$

where

$$\begin{pmatrix} \hat{\phi}_{1,[0]} \\ \hat{\phi}_{2,[0]} \\ \hat{\phi}_{3,[0]} \end{pmatrix} = \mathcal{A}\mathcal{F}_0\mathcal{G}_0\mathcal{Z}_0, \quad (3.14)$$

$$\mathcal{F}_0 = e^{\frac{ik}{2}x} \begin{pmatrix} 1 - \omega x & ia_1 x & ia_2 x \\ ia_1 x & \frac{a_1^2}{\omega^2}(1 + \omega x) + \frac{a_2^2}{\omega^2}e^{\omega x} & \frac{a_1 a_2}{\omega^2}(1 + \omega x) - \frac{a_1 a_2}{\omega^2}e^{\omega x} \\ ia_2 x & \frac{a_1 a_2}{\omega^2}(1 + \omega x) - \frac{a_1 a_2}{\omega^2}e^{\omega x} & \frac{a_2^2}{\omega^2}(1 + \omega x) + \frac{a_1^2}{\omega^2}e^{\omega x} \end{pmatrix}, \quad (3.15)$$

and

$$\mathcal{G}_0 = e^{\frac{i\vartheta}{2}t} \begin{pmatrix} 1 + \vartheta t & ia_1 \zeta t & ia_2 \zeta t \\ ia_1 \zeta t & \frac{a_1^2}{\omega^2}(1 - \vartheta t) + \frac{a_2^2}{\omega^2}\iota & \frac{a_1 a_2}{\omega^2}(1 - \vartheta t) - \frac{a_1 a_2}{\omega^2}\iota \\ ia_2 \zeta t & \frac{a_1 a_2}{\omega^2}(1 - \vartheta t) - \frac{a_1 a_2}{\omega^2}\iota & \frac{a_2^2}{\omega^2}(1 - \vartheta t) + \frac{a_1^2}{\omega^2}\iota \end{pmatrix}, \quad (3.16)$$

with

$$\vartheta = 6\omega^3 - 6ik\omega^2 - 3k^2\omega, \quad \zeta = -6\omega^2 + 6ik\omega + 3k^2, \quad \iota = e^{(-4\omega^3 + 3ik\omega^2 + 3k^2\omega)t}. \quad (3.17)$$

- (1) The first-type first-order semi-rational solutions. Fixing $a_1 = a_2 = \mu_1 = \mu_2 = \mu_3 = 1$, one can arrive at the rational solution, which is degenerated from the semi-rational solution. Besides, both components are the fundamental rogue waves. The corresponding figures are neglected here. If we choose $0 < |k| < 1$, the rogue wave possesses the curve shape, as shown in Figure 1. The amplitude of the curve rogue wave is still about 3. However, different from the fundamental rogue wave, the curve rogue wave has two maximum values.
- (2) The second-type first-order semi-rational solutions. If one of the parameters a_1 and a_2 is equal to zero, one can get the second-type semi-rational solutions among the bright/dark/curve rogue wave, one dark/bright soliton in Figures 2–6. When the value of $|\mu_2|$ increases, the rogue waves are far away from the soliton in Figures 2–3. Interestingly, in Figure 3(b), the peak difference between the rogue wave and the plane is almost zero. In other words, the energy to generate the rogue wave is small. For analyzing clearly the explicit collision processes in the semi-rational solutions, the plane evolution plots of the interactional processes at different times are exhibited in Figure 4. In Figure 4, one can find that if $t < 0$, the solitons in u_1 and u_2 components are a dark and bright soliton respectively. Nevertheless, when $t = 0$, suddenly, out of nowhere, a rogue wave appears. Then, the rogue wave disappears, and the soliton continues moving ahead whose amplitudes and velocities do not change after the collision. We call this process elastic. On the other hand, under the condition $\mu_2 \neq \mu_3$, the bright rogue waves transform into the dark rogue waves

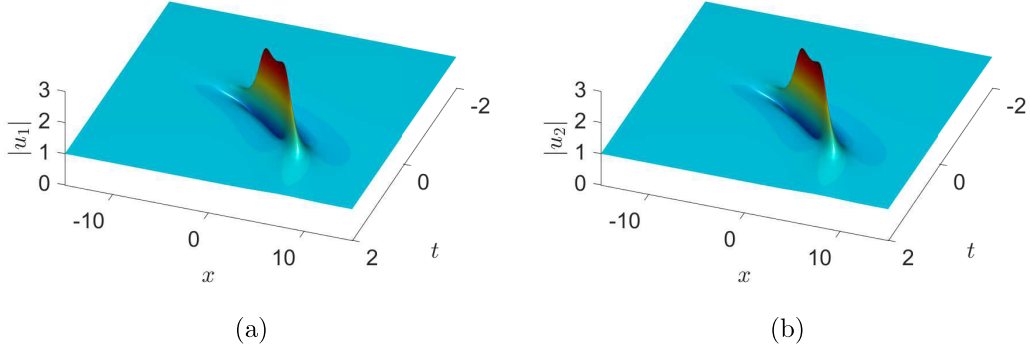


FIGURE 1. The curve rogue waves with $a_1 = 1$, $a_2 = 1$, $k = \frac{1}{2}$, $\mu_1 = 1$, $\mu_2 = 1$, $\mu_3 = 1$.

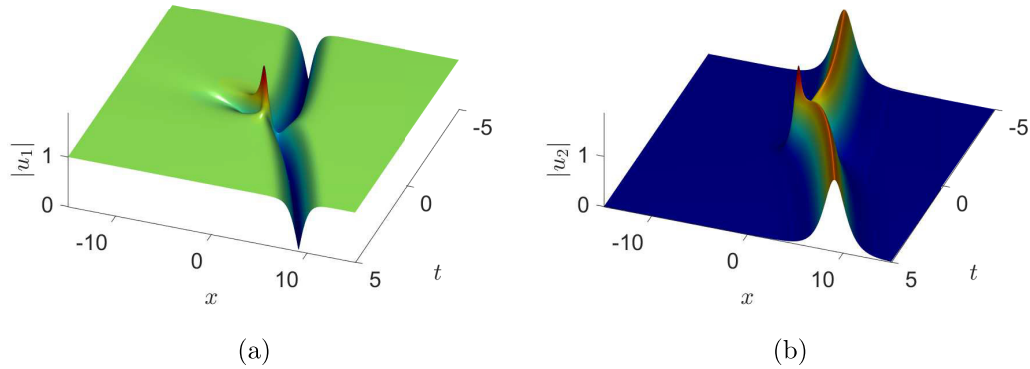


FIGURE 2. The second-type first-order semi-rational solutions with $a_1 = 1$, $a_2 = 0$, $k = 1$, $\mu_1 = 1$, $\mu_2 = 1$, $\mu_3 = 1$.

in Figure 5. More importantly, if $0 < |k| < 1$, the structure of the fundamental rogue wave changes, that is to say, the curve rogue wave appears in Figure 6.

- (3) The third-type first-order semi-rational solutions. Taking $a_1 a_2 \neq 0$, one can get the third-type semi-rational solutions where the bright/dark/curve rogue wave interplays with one breather. As shown in Figures 7–10, the first-order rogue wave and one breather separate for both components. If $a_1 = a_2 = k = 1$, the structures of the breathers in the u_1 and u_2 components are similar, as seen in Figure 7. But the breathers in Figure 8(a), (b) are very different. In Figure 8(a), the dark breather appears. It is found that the breathers' amplitudes on the plane are lower than the ones under the plane. Nevertheless, the breathers' amplitudes are inverse in Figure 8(b). By the same token, if $0 < |k| < 1$, the fundamental rogue wave changes into the curve rogue wave in Figures 9 and 10. Moreover, $\mu_2 \neq \mu_3$ yields that the bright rogue wave changes into the dark rogue wave in Figure 10(a) and the amplitude of rogue wave in u_2 component becomes from almost zero to three in Figure 10(b).

Thereinafter, one will give the other interesting magnificent patterns, namely, the second-order semi-rational solutions

$$\begin{pmatrix} u_{1,[2]} \\ u_{2,[2]} \end{pmatrix} = \begin{pmatrix} u_{1,[1]} \\ u_{2,[1]} \end{pmatrix} - \frac{(\lambda_1 - \lambda_1^*) \hat{\phi}_{1,[1]}}{|\hat{\phi}_{1,[1]}|^2 + |\hat{\phi}_{2,[1]}|^2 + |\hat{\phi}_{3,[1]}|^2} \begin{pmatrix} \hat{\phi}_{2,[1]} \\ \hat{\phi}_{3,[1]} \end{pmatrix}, \quad (3.18)$$

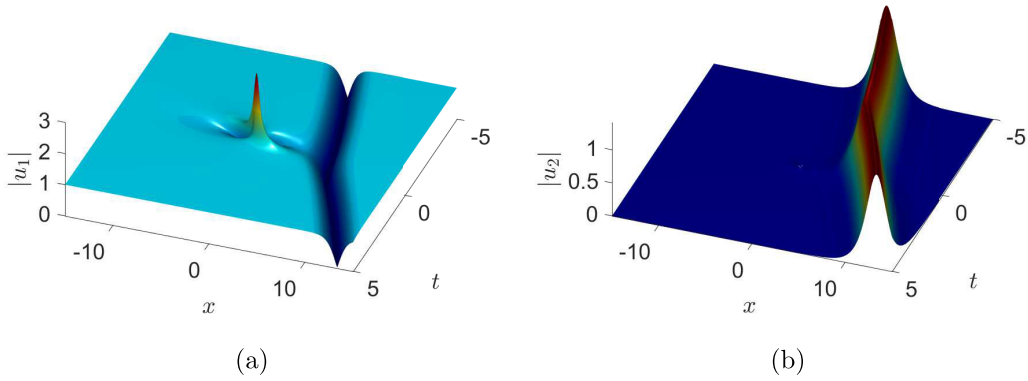


FIGURE 3. The second-type first-order semi-rational solutions with $a_1 = 1$, $a_2 = 0$, $k = 1$, $\mu_1 = 1$, $\mu_2 = 100$, $\mu_3 = 1$.

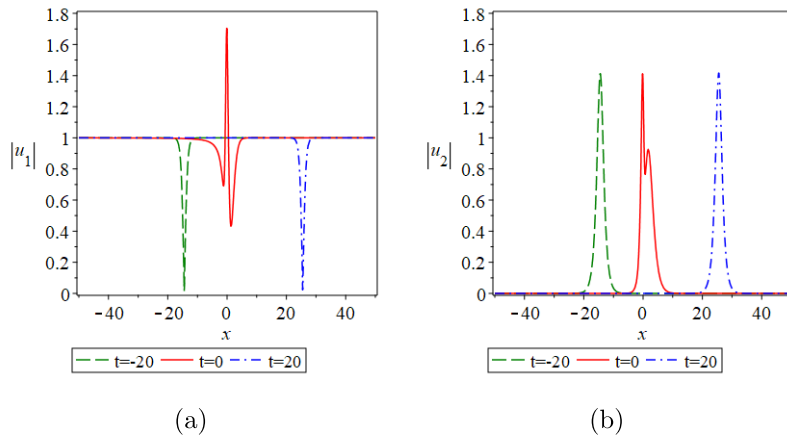


FIGURE 4. The plane evolution plots of the interactional process in the second-type first-order semi-rational solutions with the same parameters as Figure 3.

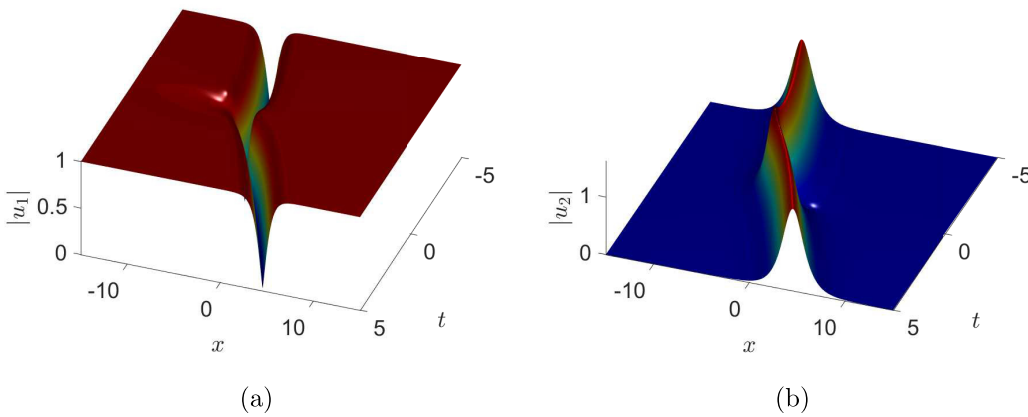


FIGURE 5. The second-type first-order semi-rational solutions with $a_1 = 1$, $a_2 = 0$, $k = 1$, $\mu_1 = 1$, $\mu_2 = 1$, $\mu_3 = 100$.

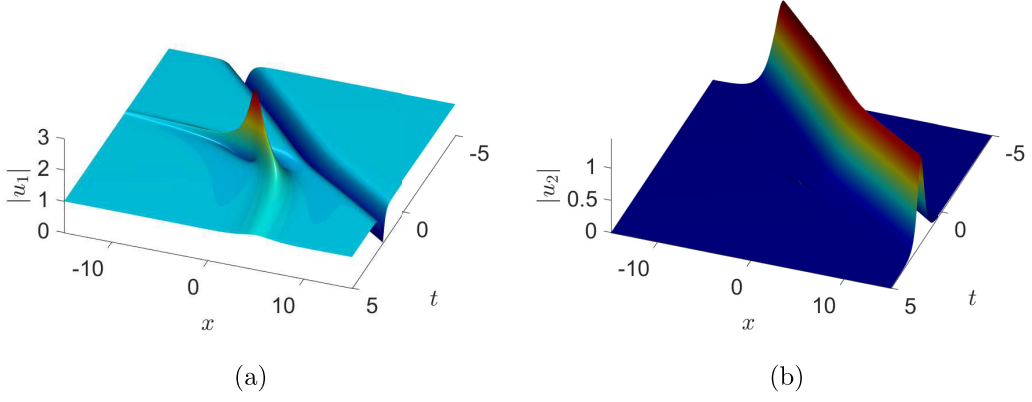


FIGURE 6. The second-type first-order semi-rational solutions with $a_1 = 1$, $a_2 = 0$, $k = \frac{1}{2}$, $\mu_1 = 1$, $\mu_2 = 100$, $\mu_3 = 1$.

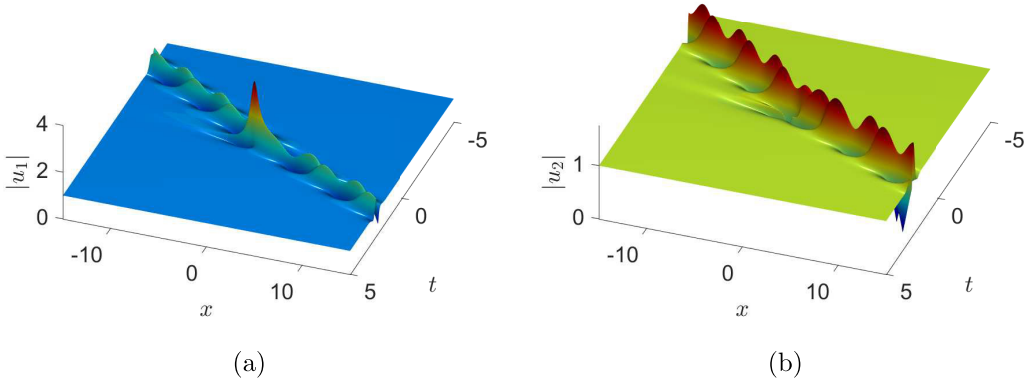


FIGURE 7. The third-type first-order semi-rational solutions with $a_1 = 1$, $a_2 = 1$, $k = 1$, $\mu_1 = 1$, $\mu_2 = 100$, $\mu_3 = 1$.

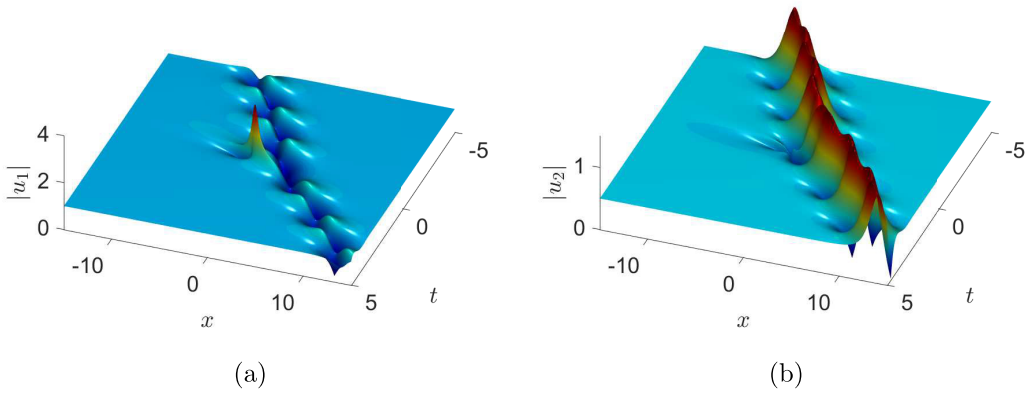


FIGURE 8. The third-type first-order semi-rational solutions with $a_1 = 1$, $a_2 = \frac{1}{2}$, $k = 1$, $\mu_1 = 1$, $\mu_2 = 100$, $\mu_3 = 1$.

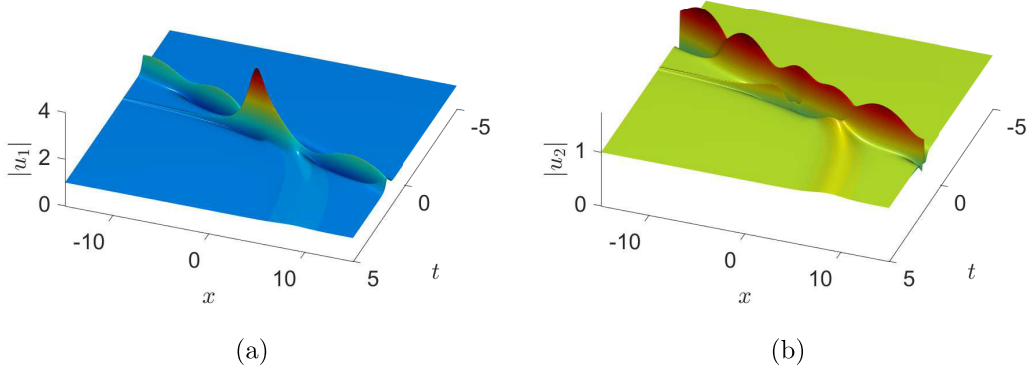


FIGURE 9. The third-type first-order semi-rational solutions with $a_1 = 1$, $a_2 = 1$, $k = \frac{1}{2}$, $\mu_1 = 1$, $\mu_2 = 100$, $\mu_3 = 1$.

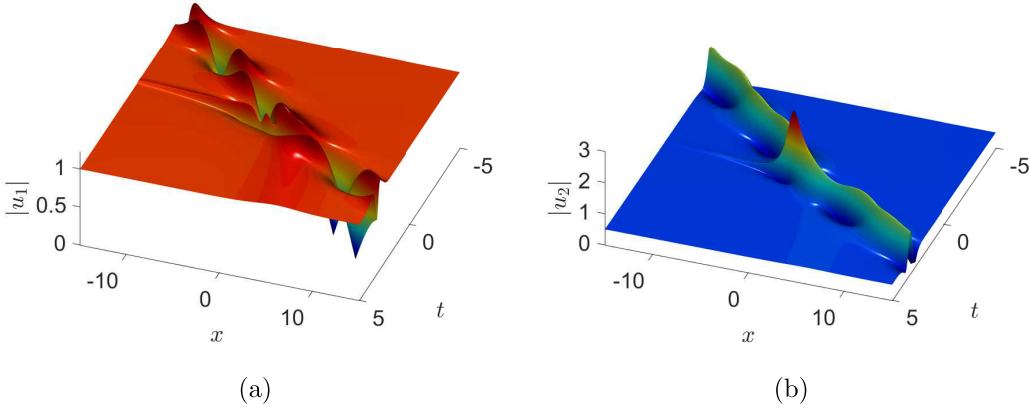


FIGURE 10. The third-type first-order semi-rational solutions with $a_1 = 1$, $a_2 = \frac{1}{2}$, $k = \frac{2}{3}$, $\mu_1 = 1$, $\mu_2 = 100$, $\mu_3 = 1000$.

where

$$\begin{pmatrix} \hat{\phi}_{1,[1]} \\ \hat{\phi}_{2,[1]} \\ \hat{\phi}_{3,[1]} \end{pmatrix} = D[1]\Psi_1 + (k + 2i\omega)\Psi_0, \quad (3.19)$$

$$D[1] = 4i\omega \left(I - \frac{\hat{\Phi}_0 \hat{\Phi}_0^\dagger}{\hat{\Phi}_0^\dagger \hat{\Phi}_0} \right),$$

$$\Psi_1 = \mathcal{A}(\mathcal{F}_1 \mathcal{G}_0 \mathcal{Z}_0 + \mathcal{F}_0 \mathcal{G}_1 \mathcal{Z}_0 + \mathcal{F}_0 \mathcal{G}_0 \mathcal{Z}_1),$$

$$\mathcal{F}_1 = e^{\frac{ik}{2}x} \begin{pmatrix} \Gamma_1 & ia_1 \Gamma_2 x^3 & ia_2 \Gamma_2 x^3 \\ ia_1 \Gamma_2 x^3 & \frac{a_1^2}{\omega^2} \Gamma_3 + \frac{a_2^2}{\omega^2} (\omega - \frac{ik}{2}) x e^{\omega x} & \frac{a_1 a_2}{\omega^2} \Gamma_3 - \frac{a_1 a_2}{\omega^2} (\omega - \frac{ik}{2}) x e^{\omega x} \\ ia_2 \Gamma_2 x^3 & \frac{a_1 a_2}{\omega^2} \Gamma_3 - \frac{a_1 a_2}{\omega^2} (\omega - \frac{ik}{2}) x e^{\omega x} & \frac{a_2^2}{\omega^2} \Gamma_3 + \frac{a_1^2}{\omega^2} (\omega - \frac{ik}{2}) x e^{\omega x} \end{pmatrix}, \quad (3.20)$$

and

$$\mathcal{G}_1 = e^{\frac{i\pi}{2}t} \begin{pmatrix} \Upsilon_1 & a_1 \Upsilon_2 t & a_2 \Upsilon_2 t \\ a_1 \Upsilon_2 t & \frac{a_1^2}{\omega^2} \Upsilon_3 + \frac{a_2^2}{\omega^2} \Upsilon_4 & \frac{a_1 a_2}{\omega^2} \Upsilon_3 - \frac{a_1 a_2}{\omega^2} \Omega_4 \\ a_2 \Upsilon_2 t & \frac{a_1 a_2}{\omega^2} \Upsilon_3 - \frac{a_1 a_2}{\omega^2} \Upsilon_4 & \frac{a_2^2}{\omega^2} \Upsilon_3 + \frac{a_1^2}{\omega^2} \Upsilon_4 \end{pmatrix}, \quad (3.21)$$

with

$$\Gamma_1 = -\frac{\omega^3}{3}x^3 + \frac{ik\omega^2}{6}x^3 + \omega^2x^2 - \frac{ik\omega}{2}x^2 - \omega x + \frac{ik}{2}x,$$

$$\Gamma_2 = \frac{\omega^2}{3} - \frac{ik\omega}{6},$$

$$\Gamma_3 = \frac{\omega^3}{3}x^3 - \frac{ik\omega^2}{6}x^3 + \omega^2x^2 - \frac{ik\omega}{2}x^2 + \omega x - \frac{ik}{2}x,$$

$$\begin{aligned} \Upsilon_1 = & \frac{1}{-4\omega^2 + 4ik\omega + 2k^2} (9(-32t^3\omega^{11} + 144ikt^3\omega^{10} + 320k^2t^3\omega^9 + (-448ik^3t^3 - 16t^2)\omega^8 \\ & + (-432k^4t^3 + 56ikt^2)\omega^7 + (296ik^5t^3 + 96k^2t^2)\omega^6 + (144k^6t^3 - 100ik^3t^2 - \frac{56}{9}t)\omega^5 \\ & + (-48ik^7t^3 - 64k^4t^2 + \frac{44}{3}ikt)\omega^4 + (-10k^8t^3 + 30ik^5t^2 + \frac{140}{9}k^2t)\omega^3 + k^3(ik^6t^3 + 8k^3t^2 - \frac{80}{9}it)\omega^2 \\ & + (-ik^7t^2 - \frac{8}{3}k^4t)\omega + \frac{1}{3}ik^5t), \end{aligned}$$

$$\begin{aligned} \Upsilon_2 = & -72it^2\omega^8 - 252t^2k\omega^7 + 432it^2k^2\omega^6 + 450t^2k^3\omega^5 - 306it^2k^4\omega^4 - 135t^2k^5\omega^3 + 36it^2k^6\omega^2 \\ & - 8i\omega^2 - 10k\omega + \frac{9}{2}t^2k^7\omega - 3ik^2, \end{aligned}$$

$$\begin{aligned} \Upsilon_3 = & \frac{1}{-4\omega^2 + 4ik\omega + 2k^2} (9(32t^3\omega^{11} - 144ikt^3\omega^{10} - 320k^2t^3\omega^9 + (448ik^3t^3 - 16t^2)\omega^8 \\ & + (432k^4t^3 + 56ikt^2)\omega^7 + (-296ik^5t^3 + 96k^2t^2)\omega^6 + (-144k^6t^3 - 100ik^3t^2 + \frac{56}{9}t)\omega^5 \\ & + (48ik^7t^3 - 64k^4t^2 - \frac{44}{3}ikt)\omega^4 + (10k^8t^3 + 30ik^5t^2 - \frac{140}{9}k^2t)\omega^3 + k^3(-ik^6t^3 + 8k^3t^2 + \frac{80}{9}it)\omega^2 \\ & + (-ik^7t^2 + \frac{8}{3}k^4t)\omega - \frac{1}{3}ik^5t), \end{aligned}$$

$$\Upsilon_4 = (-48\omega^5 + 120ik\omega^4 + 132k^2\omega^3 - 78ik^3\omega^2 - 24k^4\omega + 3ik^5)te^{(-4\omega^3 + 3ik\omega^2 + 3k^2\omega)t}.$$

Thereafter, we show three kinds of second-order semi-rational solutions.

- (1) The first-type second-order semi-rational solutions. Under $a_1 = a_2 = l_1 = l_3 = 1$, the second-order semi-rational solutions degenerate to the second-order rogue waves which possess two forms: the fundamental and triangular pattern. Similarly, we do not show the plots here.
- (2) The second-type second-order semi-rational solutions. If $a_1 \neq 0$ and $a_2 = 0$, one can obtain the semi-rational solutions coexisting with the second-order rogue waves, two dark and bright solitons in Figures 11–12. If $R_j = 0$ and $S_j = 0$, the interactional solutions are the fundamental second-order rogue waves with two dark and bright solitons in Figure 11. Similarly, rogue waves are not apparent on the bright solitons background in Figure 11(b). When choosing $R_j = 0$ and $S_2 \neq 0$, the pattern of the second-order rogue waves becomes triangular.

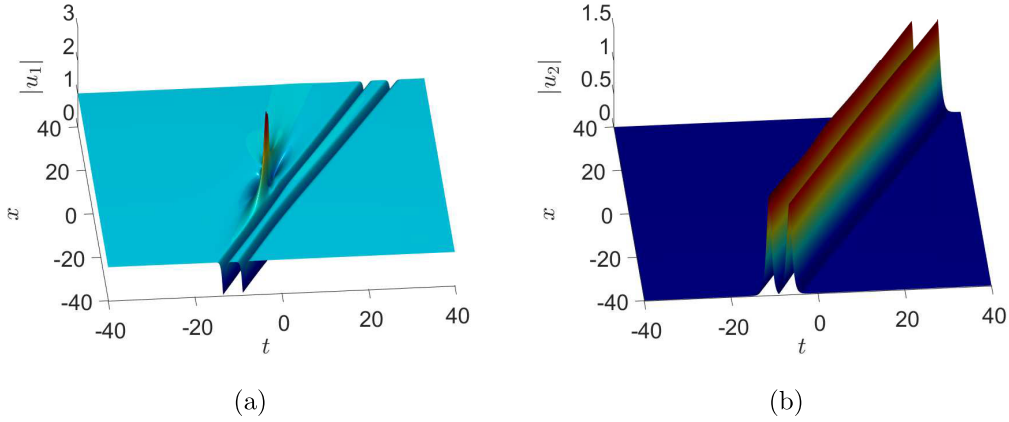


FIGURE 11. The second-type second-order semi-rational solutions with $a_1 = 1$, $a_2 = 0$, $k = 1$, $p_1 = 200$, $p_2 = 1$, $p_3 = 10$, $R_j = 0$, $S_j = 0$.

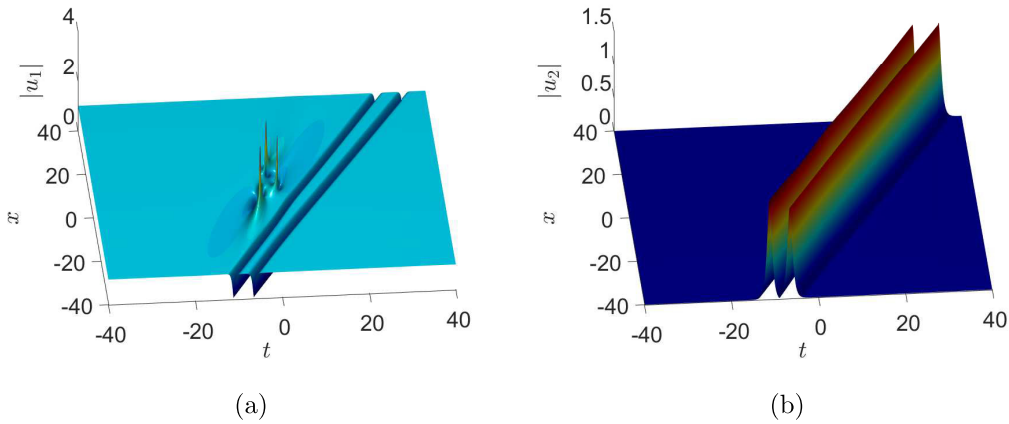


FIGURE 12. The second-type second-order semi-rational solutions with the same parameters as Figure 11 except that $p_1 = 20000$, $p_3 = 10000$, $S_2 = 50$.

- (3) The third-type second-order semi-rational solutions. If $a_1 a_2 \neq 0$, the second-order semi-rational solutions consist of the second-order rational solutions and breathers in Figures 13–14. Choosing $R_j = 0$, $S_j = 0$, the fundamental second-order rogue waves and breathers coexist in both u_1 and u_2 components. Supposing $S_2 \neq 0$, rogue waves will become the triangular.

In the same manner, more higher-order semi-rational solutions of equation (1.1) can be generated by the DDT method. Compared with the low-order cases, we can also classify higher-order cases as three types: (1) N -order rational solutions; (2) N -order rational solutions interact with N -solitons; (3) N -order rational solutions interact with N -breathers. On the one hand, the values of the parameters a_1 and a_2 influence the types of the localized solutions. On the other hand, changing the free vector parameter \mathcal{Z} results in the diverse patterns of rogue waves.

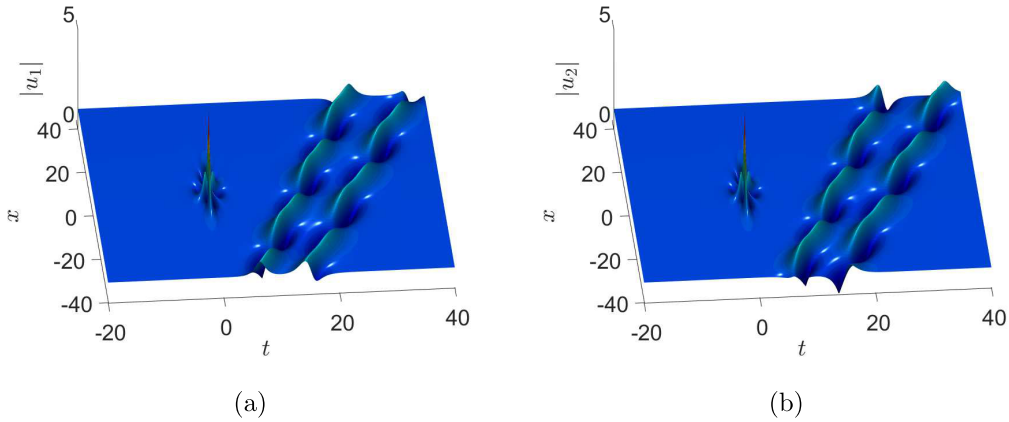


FIGURE 13. The third-type second-order semi-rational solutions with the parameters $a_1 = 1$, $a_2 = 1$, $k = 1$, $p_1 = 500$, $p_2 = 1$, $p_3 = 100$, $R_j = 0$, $S_j = 0$.

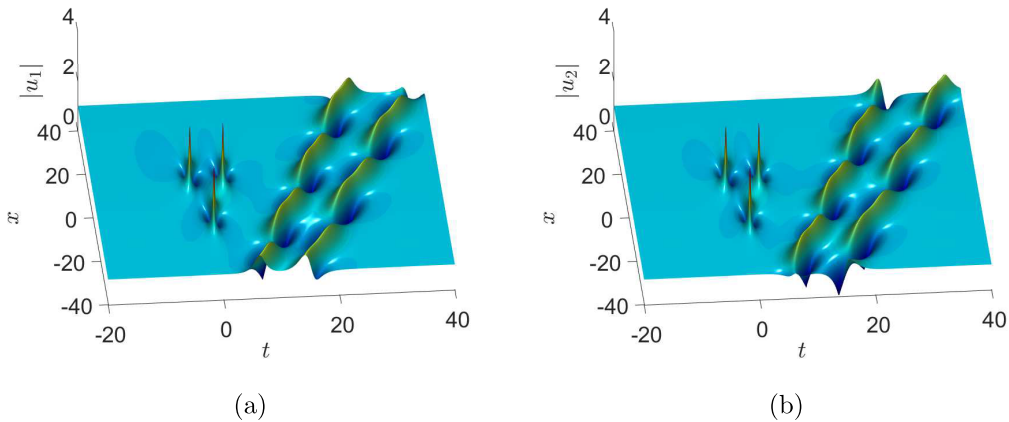


FIGURE 14. The third-type second-order semi-rational solutions with the same parameters as Figure 13 except that $p_1 = 25000$, $p_3 = 20000$, $S_2 = 100$.

4. CONCLUSION

We definitely exhibit a variety of semi-rational solutions of the ccmKdV equation resorting to a novel method, namely, the DDT method. Moreover, different from other researches, we consider an initial solution with the distance and time such that curve rouge waves can be obtained. Through the adjustments of the parameters, we achieve the three categories of semi-rational solutions. Continuing the DDT process, more complicated and interesting solutions can be obtained, which possess richer dynamics. Based on the matrix exponential function, we construct the semi-rational solutions whose propagation property is extremely distinct from the others. We expect that our results are advantageous to understand more complicated physical phenomena.

Acknowledgements. This work is supported by the National Natural Science Foundation of China (No. 11371326 and No. 11975145).

REFERENCES

- [1] N. Akhmediev, A. Ankiewicz and M. Taki, Waves that appear from nowhere and disappear without a trace. *Phys. Lett. A* **373** (2009) 675–678.
- [2] N. Akhmediev and V.I. Korneev, Modulation instability and periodic solutions of the nonlinear Schrödinger equation. *Theor. Math. Phys.* **69** (1986) 1089–1093.
- [3] Y.V. Bludov, V.V. Konotop and N. Akhmediev, Matter rogue waves. *Phys. Rev. A* **80** (2009) 033610.
- [4] A. Degasperis and S. Lombardo, Multicomponent integrable wave equations: I. Darboux-dressing transformation. *J. Phys. A: Math. Theor.* **40** (2007) 961–977.
- [5] A. Degasperis and S. Lombardo, Multicomponent integrable wave equations: II. Soliton solutions. *J. Phys. A: Math. Theor.* **42** (2009) 2467–2480.
- [6] K. Dysthe, H.E. Krogstad and P. Müller, Oceanic rogue waves. *Annu. Rev. Fluid Mech.* **40** (2008) 287–310.
- [7] H.A. Erbay, Nonlinear transverse waves in a generalized elastic solid and the complex modified Korteweg-de Vries equation. *Phys. Scr.* **58** (1998) 9–14.
- [8] X.G. Geng, Y.Y. Zhai and H.H. Dai, Algebro-geometric solutions of the coupled modified Korteweg-de Vries hierarchy. *Adv. Math.* **263** (2014) 123–153.
- [9] B.L. Guo, L.M. Ling, Q.P. Liu and C.F. Wu, Nonlinear Schrödinger equation: generalized Darboux transformation and rogue wave solutions. *Phys. Rev. E* **85** (2012) 026607.
- [10] J.S. He, L.H. Wang, L.J. Li, K. Porsezian and R. Erdélyi, Few-cycle optical rogue waves: complex modified Korteweg-de Vries equation. *Phys. Rev. E* **89** (2014) 062917.
- [11] A.H. Khater, O.H. El-Kalaawy and D.K. Callebaut, Bäcklund transformations and exact solutions for Alfvén solitons in a relativistic electron-positron plasma. *Phys. Scr.* **58** (1988) 545.
- [12] B. Kibler, J. Fatome, C. Finot, G. Millot and F. Dias, The Peregrine soliton in nonlinear fibre optics. *Nat. Phys.* **6** (2010) 790.
- [13] E.A. Kuznetsov, Solitons in a parametrically unstable plasma. *Akad. Nauk SSSR Dokl.* **236** (1977) 575–577.
- [14] H. Leblond, P. Grelu and D. Mihalache, Models for supercontinuum generation beyond the slowly-varying-envelope approximation. *Phys. Rev. A* **90** (2014) 053816.
- [15] L.M. Ling, B.L. Guo and L.C. Zhao, High-order rogue waves in vector nonlinear Schrödinger equations. *Phys. Rev. E* **89** (2014) 041201.
- [16] K.E. Lonngren, Ion acoustic soliton experiments in a plasma. *Opt. Quant. Electron.* **30** (1998) 615.
- [17] Y. Lou, Y. Zhang and R.S. Ye, Modulation instability, higher-order rogue waves and dynamics of the Gerdjikov-Ivanov equation. *Wave Motion* **106** (2021) 102795.
- [18] Y. Lou, Y. Zhang, R.S. Ye and M. Li, Solitons and dynamics for the integrable nonlocal pair-transition-coupled nonlinear Schrödinger equation. *Appl. Math. Comput.* **409** (2021) 126417.
- [19] W.X. Ma, Riemann-Hilbert problems and N -soliton solutions for a coupled mKdV system. *J. Geom. Phys.* **132** (2018) 45–54.
- [20] G. Mu, Z.Y. Qin and R. Grimshaw, Dynamics of rogue waves on a multisoliton background in a vector nonlinear Schrödinger equation. *SIAM J. Appl. Math.* **75** (2015) 1–20.
- [21] N.V. Priya, M. Senthilvelan and M. Lakshmanan, Akhmediev breathers, Ma solitons, and general breathers from rogue waves: a case study in the Manakov system. *Phys. Rev. E* **88** (2013) 022918.
- [22] D.R. Solli, C. Ropers, P. Koonath *et al.*, Optical rogue waves. *Nature* **450** (2007) 1054–1057.
- [23] X. Wang, Y. Li and Y. Chen, Generalized Darboux transformation and localized waves in coupled Hirota equations. *Wave Motion* **51** (2014) 1149–1160.
- [24] R. Wang, Y. Zhang, X.T. Chen and R.S. Ye, The rational and semi-rational solutions to the Hirota-Maccari system. *Nonlinear Dyn.* **100** (2020) 2767–2778.
- [25] T. Xu and G.L. He, Higher-order interactional solutions and rogue wave pairs for the coupled Lakshmanan-Porsezian-Daniel equations. *Nonlinear Dyn.* **98** (2019) 1731–1744.
- [26] T. Xu and G.L. He, The coupled derivative nonlinear Schrödinger equation: conservation laws, modulation instability and semirational solutions. *Nonlinear Dyn.* **100** (2020) 2823–2837.
- [27] Z.Y. Yan, Vector financial rogue waves. *Phys. Lett. A* **375** (2011) 4274–4279.
- [28] R.S. Ye, Y. Zhang, Q.Y. Zhang and X.T. Chen, Vector rational and semi-rational rogue wave solutions in the coupled complex modified Korteweg-de Vries equations. *Wave Motion* **92** (2019) 102425.
- [29] Y.Y. Zhai, T. Ji and X.G. Geng, Coupled derivative nonlinear Schrödinger III equation: Darboux transformation and higher-order rogue waves in a two-mode nonlinear fiber. *Appl. Math. Comput.* **411** (2021) 126551.
- [30] Y. Zhang, R.S. Ye and W.X. Ma, Binary Darboux transformation and soliton solutions for the coupled complex modified Korteweg-de Vries equations. *Math. Meth. Appl. Sci.* **43** (2019) 613–627.

- [31] Y. Zhang, J.W. Yang, K.W. Chow *et al.*, Solitons, breathers and rogue waves for the coupled Fokas-Lenells system via Darboux transformation. *Nonlinear Anal. RWA* **33** (2017) 237–252.

Subscribe to Open (S2O)

A fair and sustainable open access model



This journal is currently published in open access under a Subscribe-to-Open model (S2O). S2O is a transformative model that aims to move subscription journals to open access. Open access is the free, immediate, online availability of research articles combined with the rights to use these articles fully in the digital environment. We are thankful to our subscribers and sponsors for making it possible to publish this journal in open access, free of charge for authors.

Please help to maintain this journal in open access!

Check that your library subscribes to the journal, or make a personal donation to the S2O programme, by contacting subscribers@edpsciences.org

More information, including a list of sponsors and a financial transparency report, available at: <https://www.edpsciences.org/en/math-s2o-programme>